Advances in Intelligent Systems Research (AISR), volume 151
2018 International Conference on Computer Modeling, Simulation and Algorithm (CMSA 2018)

Teeth Category Classification via Hu Moment Invariant and Extreme Learning Machine

Zhi Li[1], Ting Guo[2,*], Fangzhou Bao[3] and Rodney Payne[4]
[1]Department of Stomatology, Jinling Hospital, School of Medicine, Nanjing University, 305 East Zhongshan Road, 210002 Nanjing, Jiangsu, China
[2]Nanjing Stomatological Hospital, Medical School of Nanjing University, Nanjing, Jiangsu, China
[3]Jiangsu Key Laboratory of 3D Printing Equipment and Manufacturing, Nanjing, Jiangsu 210042, China
[4]John E. Walker Department of Economics, Clemson University, Clemson, SC 29634, USA
[*]Corresponding author

***Abstract*—To improve the computer-assisted diagnosis and decision in dentistry, we tested a new method combining Hu moment invariant (HMI) method and extreme learning machine (ELM) to implement the teeth classification in cross-section image of Cone Beam Computed Tomography (CBCT). 160 images were analyzed and 4 categories were recognized. The results showed the sensitivities of incisors, canine, premolar, and molars were 78.25± 6.02%, 78.00± 5.99%, 79.25± 7.91%, and 78.75± 5.17%, better than ANN statistical-significantly.**

Keywords—teeth classification; Hu moment invariant; extreme learning machine

I. INTRODUCTION

With the progress of computer technology, artificial intelligence has penetrated into every field of knowledge. In medicine, machine learning allows medical workers to process huge image data and recognize quantitative features or areas, which provides reference and theory for diagnosis, and improve diagnosis efficiency, accuracy and repeatability. Artificial intelligence may help us in prognosticating the disease and guiding in clinical diagnosis and treatment.

Teeth is an important organ in dentistry. According to the morphological function of the teeth, it can be divided into four categories: incisor (incisor, incisor), canine, premolar (first premolar, second premolar), molar (first molar, second molar, Third molars). Those different morphological characteristics reflect in the imaging data, such as Cone Beam Computed Tomography (CBCT), which can observe the tooth shape, size, location and the relationship with the adjacent teeth at any angle, with low radiation and high spatial resolution [1]. Compared with any other imaging methods, CBCT produces high-quality images for hard tissues, especially dental tissues [2]. Thus, CBCT achieves ubiquity in the diagnosis of oral diseases.

Teeth classification is an important component in the computer-assisted diagnosis and decision. In order to recognize tooth classification, researchers have proposed various machine learning algorithms. Yoke-San introduced a classification system based on the iterative closest point algorithm (ICP) to handle tooth crown segmented from scanned dental casts and entire single tooth reconstructed from CBCT images [3]. Al-sherif identified 622 bitewing dental images by using Orthogonal Locality Preserving Projection (OLPP) algorithm to assign an initial class, then number the teeth based on teeth neighborhood rules [4]. Pushparaj used Support Vector Machine to classify the teeth and utilized template matching algorithm to assign teeth number by panoramic images [5]. Tangel presented a fuzzy inference system for dental classification by 78 periapical radiographs, analyzed teeth based on multiple criteria such as area/perimeter ratio and width/height ratio [6].

In this study, we tested a new method combining Hu moment invariant (HMI) method and extreme learning machine (ELM) to implement the teeth classification in cross-section image of CBCT. This paper follows the standard of computer vision [7-9] and medical image processing [10-12]. Four categories are recognized: central incisor, lateral incisor, canine and premolar.

II. METHODOLOGY

A. Hu Moment Invariant

Currently there are numerous feature extraction methods, for example, Fourier transform [13-16], wavelet analysis [17-19], and so on. Moment invariant was proposed by Hu in 1962, with invariant character for translation, rotation and scale, and was widely applied in pattern recognition. $F(x, y)$ is a piecewise continuous therefore bounded function, whose two-dimensional $(p + q)$ moment is defined as:

$$M_{pq} = \int_{-\infty}^{\infty}\int_{-\infty}^{\infty} x^p y^q f(x,y)dxdy,\ p,q = 0,1,2 \quad (1)$$

The double moment sequence (M_{pq}) is uniquely determined by $f(x,y)$ And vice versa. (p + q) order center moments are defined as:

$$C_{pq} = \int_{-\infty}^{\infty}\int_{-\infty}^{\infty} (x-x_1)^p (y-y_1)^q f(x,y)dxdy \quad (2)$$

The components of the centroid are as follows:

$$x_1 = {M_{10}}/{M_{00}} \quad (3)$$

$$y_1 = M_{01} / M_{00} \quad (4)$$

If $f(x, y)$ is a digital image, then we have integrals instead of sums, the Hu moments(1) and corresponding center moments(2) becomes:

$$M_{pq} = \sum\sum x^p y^q f(x, y) \quad (5)$$

$$C_{pq} = \sum\sum (x - x_1)^p (y - y_1)^q f(x, y) \quad (6)$$

The center moments are C_{pq} shift invariant, in order to obtain the scale invariance, we normalize the central moments as:

$$N_{pq} = C_{pq} / C_{00}^{(1+p+q/2)}, \; p + q = 2,3,4 \quad (7)$$

Hu applied the algebraic invariant theory to the above scale invariants and constructed the following seven invariants, which were linear combinations of the second and third order central moments:

$$I_1 = N_{20} + N_{02} \quad (8)$$

$$I_2 = (N_{20} + N_{02})^2 = 4N_{11}^2 \quad (9)$$

$$I_3 = (N_{30} + 3N_{12})^2 + (3N_{21} - N_{03})^2 \quad (10)$$

$$I_4 = (N_{30} + N_{12})^2 + (N_{21} + N_{03})^2 \quad (11)$$

$$I_5=(N_{30}-3N_{12})(N_{30}+N_{12})[(N_{30}+N_{12})^2-3(N_{21}+N_{03})^2]+(3N_{21}-N_{03})(N_{21}+N_{03})[3(N_{30}+3N_{12})^2-(N_{21}+N_{03})^2] \quad (12)$$

$$I_6 = (N_{20} - N_{02})[(N_{30} + N_{12})^2 - (N_{21} + N_{03})^2] + 4N_{11}(N_{30} + N_{12})(N_{21} + N_{03}) \quad (13)$$

$$I_7=(3N_{21}-N_{03})(N_{30}+N_{12})[(N_{30}+N_{12})^2-3(N_{21}+N_{03})^2]-(N_{30}-3N_{12})(N_{21}+N_{03})[3(N_{30}+N_{12})^2-(N_{21}+N_{03})^2 \quad (14)$$

Generally, These *Hu moment* invariants (I_1~I_7) are the invariant characteristics of the target.

B. Extreme Learning Machine

ELM is a single-hidden layer feedforward neural network (SLFNs) proposed by Huang et al. The network is constituted of input layer, hidden layer and output layer [20-22]. If the activation functions in the hidden layer are infinitely differentiable, the input weights and hidden layer biases can be randomly assigned, ELMs can be simply considered as a linear system. ELM has the fast learning speed and the universal approximation ability, which can approximate any continuous function. Scholars have proven that ELM outperforms peer classifiers, such as multilayer perceptron [23-26], support vector machine [27-29], fuzzy SVM [30-32], etc.

Given N different set of samples (I_i, D_i), where $I_i = [I_{i1}, I_{i2}, ..., I_{in}]^T \in R^n$ represents input data, and $D_i = [D_{i1}, D_{i2}, ..., D_{in}]^T \in R^m$ represents desired output. Standard SLFNs with M hidden nodes and activation function f(X) are mathematically modeled as

$$\sum_{i=1}^{M} V_i f_i(I_j) = \sum_{i=1}^{M} V_i f(W_i I_j + b_j) = O_i, i = 1,2,...N \quad (15)$$

Where $W_i = [W_{i1}, W_{i2}, ..., W_{in}]^T$ is the weight vector connecting the *i*-th hidden node and the output nodes, $V_i = [V_{i1}, V_{i2}, ..., V_{in}]^T$ is he weight vector connecting the *i*-th hidden node and the output nodes, b_i is the threshold of the *i*-th hidden node, W_iI_j is the inner product of W_i and I_j, O_j is the actual output.

If the activation function f(x) can approximate these N samples with zero error with *M* hidden nodes:

$$\sum_{j=1}^{M} \| O_j - D_j \| = 0 \quad (16)$$

Then, the exist W_i, V_i and b_i satisfy equation as:

$$\sum_{I=1}^{M} V_i f(W_i I_j + b_i) = D_j, \; j = 1,2,..., N \quad (17)$$

The above equations can be written as matrices:

$$HV=D \quad (18)$$

Where $H = \begin{bmatrix} f(W_1 I_1 + b_1) & ... & f(W_M I_1 + b_M) \\ ... & ... & ... \\ f(W_1 I_N + b_1) & ... & f(W_M I_N + b_M) \end{bmatrix}_{N \times M}$,

$V = \begin{bmatrix} V_1^T \\ ... \\ V_M^T \end{bmatrix}_{M \times m}$, $D = \begin{bmatrix} D_1^T \\ ... \\ D_N^T \end{bmatrix}_{N \times m}$

If the hidden layer output matrix of the neural network(H) and desired output (D) are known, the learning process of the ELM is to obtain the weight vector of the output(V) according to (11).

C. K-fold Cross Validation

In case of insufficient sample size, the k-fold cross-validation can make full use of the data set to test the algorithm effect. In this study, we divided the data set into 10 equal sized subsamples randomly (*k*=10). Of the 10 subsamples, we selected one as the testing set and remained the 9 subsamples as the training set. The cross-validation process was repeated 10 times, and each subsample was used once as the testing set. Finally, the results of 10 experiments (mean squared error, MSE) were averaged to produce a single estimation:

$$CV_{10} = 1 \Big/ \sum_{i=1}^{10} MSE_i \qquad (19)$$

We reported the mean and standard deviation of sensitivity of all four classes. The higher the value is, the better the performance is.

III. Dataset

In our experiment, the CBCT images of teeth are used for reducing the damage to the human body in the process of imaging. In total, we have a 160-image dataset, which contains 40 incisors, 40 canines, 40 premolars, and 40 molars. Figure I shows the samples of our dataset.

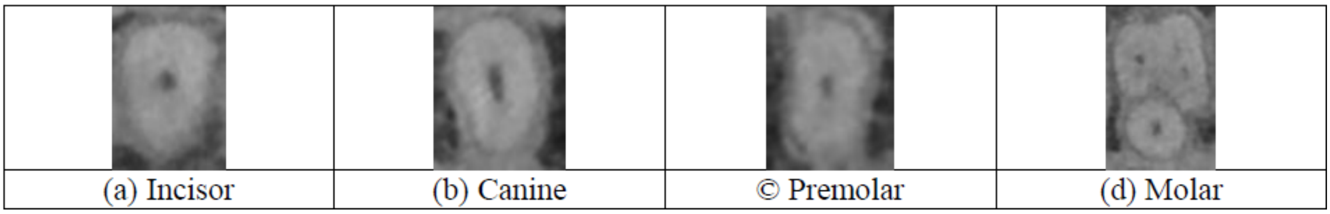

FIGURE I. SAMPLES OF OUR DATASET

IV. Results and Discussions

The 10 repetitions of 10-fold cross validation of our HMI_ELM method was shown in Table I. Here the sensitivities of incisors, canine, premolar, and molars are 78.25± 6.02%, 78.00± 5.99%, 79.25± 7.91%, and 78.75± 5.17%.

TABLE I. CROSS VALIDATION RESULTS OF OUR METHOD

Run	Incisor	Canine	Premolar	Molar
R1	72.50	75.00	82.50	82.50
R2	72.50	70.00	82.50	77.50
R3	82.50	85.00	60.00	85.00
R4	70.00	80.00	87.50	75.00
R5	90.00	72.50	75.00	85.00
R6	80.00	85.00	77.50	77.50
R7	80.00	80.00	80.00	72.50
R8	77.50	77.50	82.50	75.00
R9	75.00	85.00	77.50	85.00
R10	82.50	70.00	87.50	72.50
Average	78.25± 6.02	78.00± 5.99	79.25± 7.91	78.75± 5.17

Next, we compared our ELM method with artificial neural network (ANN) method [33]. The ANN results were listed in Table II. We can observe the ANN [33] method achieved sensitivities results of the four classes as 76.00± 3.94%, 75.00± 5.53%, 76.00± 6.89%, and 75.25± 2.49%, respectively.

TABLE II. CROSS VALIDATION RESULTS OF ANN

Run	Incisor	Canine	Premolar	Molar
R1	72.50	80.00	72.50	75.00
R2	77.50	75.00	82.50	72.50
R3	80.00	77.50	75.00	75.00
R4	77.50	65.00	85.00	75.00
R5	80.00	67.50	85.00	72.50
R6	77.50	77.50	62.50	80.00
R7	67.50	77.50	75.00	77.50
R8	77.50	80.00	72.50	75.00
R9	72.50	80.00	77.50	72.50
R10	77.50	70.00	72.50	77.50
Average	76.00± 3.94	75.00± 5.53	76.00± 6.89	75.25± 2.49

A comparison plot was shown below for better visual quality in Figure II. It is clear observed that this proposed method achieved better result than ANN [33] statistical-significantly. This again shows the effectiveness of our proposed method, and the superiority of our method to traditional ANN method.

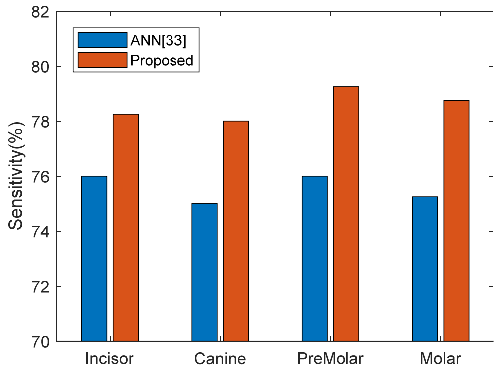

FIGURE II. COMPARISON RESULT

V. Conclusion

In this study, a novel approach for classification of CBCT teeth images combining Hu moment invariant (HMI) method and extreme learning machine (ELM) had been proposed and implemented. This method achieved higher classification percentage than ANN method. In the future, we may apply our method to identify other diseases, including Alzheimer's disease [34], alcoholism detection [35, 36], etc.

Acknowledgement

This paper was supported by the National Natural Science Foundation of China (81500872) and Natural Science Foundation of Jiangsu Province (BK20161389).

References

[1] Al-Rawi, B., et al., *Accuracy assessment of three-dimensional surface reconstructions of teeth from Cone Beam Computed Tomography scans.* Journal of Oral Rehabilitation, 2010. **37**(5): p. 352-358

[2] Brady, E., et al., *A comparison of cone beam computed tomography and periapical radiography for the detection of vertical root fractures in nonendodontically treated teeth.* International Endodontic Journal, 2014. **47**(8): p. 735-746

[3] Wong, Y.-S., et al., *An approach for single tooth classification and identification*, in *10th Conference on Industrial Electronics and Applications (ICIEA)*. 2015, IEEE. p. 1698-1702.

[4] Al-sherif, N., G. Guo, and H.H. Ammar. *Automatic Classification of Teeth in Bitewing Dental Images Using OLPP*. in *IEEE International Symposium on Multimedia*. 2012. Irvine, CA, USA: IEEE. p. 92-95

[5] Pushparaj, V., et al. *An effective numbering and classification system for dental panoramic radiographs*. in *Fourth International Conference on*

Computing, Communications and Networking Technologies (ICCCNT). 2013. Tiruchengode, India: IEEE. p. 1-8

[6] Tangel, M.L., et al. *Dental classification for periapical radiograph based on multiple fuzzy attribute*. in *Joint IFSA World Congress and NAFIPS Annual Meeting (IFSA/NAFIPS)*. 2013. Edmonton, AB, Canada: IEEE. p. 304-309

[7] Wu, L.N., *Pattern Recognition via PCNN and Tsallis Entropy.* Sensors, 2008. **8**(11): p. 7518-7529

[8] Naggaz, N. and G. Wei, *Remote-sensing Image Classification Based on an Improved Probabilistic Neural Network.* Sensors, 2009. **9**(9): p. 7516-7539

[9] Wu, L. and G. Wei, *A New Classifier for Polarimetric SAR Images.* Progress in Electromagnetics Research, 2009. **94**: p. 83-104

[10] Wu, L.N., *Improved image filter based on SPCNN.* Science In China Series F-Information Sciences, 2008. **51**(12): p. 2115-2125

[11] Wu, L.N., *Segment-based coding of color images.* Science in China Series F-Information Sciences, 2009. **52**(6): p. 914-925

[12] Wei, G., *Color Image Enhancement based on HVS and PCNN.* SCIENCE CHINA Information Sciences, 2010. **53**(10): p. 1963-1976

[13] Liu, G., *Computer-aided diagnosis of abnormal breasts in mammogram images by weighted-type fractional Fourier transform.* Advances in Mechanical Engineering, 2016. **8**(2): Article ID. 11

[14] Li, J., *Texture Analysis Method Based on Fractional Fourier Entropy and Fitness-scaling Adaptive Genetic Algorithm for Detecting Left-sided and Right-sided Sensorineural Hearing Loss.* Fundamenta Informaticae, 2017. **151**(1-4): p. 505-521

[15] Phillips, P., *A Comprehensive Survey on Fractional Fourier Transform.* Fundamenta Informaticae, 2017. **151**(1-4): p. 1-48

[16] Cattani, C. and R. Rao, *Tea Category Identification Using a Novel Fractional Fourier Entropy and Jaya Algorithm.* Entropy, 2016. **18**(3): Article ID. 77

[17] Sun, P., *Preliminary research on abnormal brain detection by wavelet-energy and quantum-behaved PSO.* Technology and Health Care, 2016. **24**(s2): p. S641-S649

[18] Yang, M., *Dual-Tree Complex Wavelet Transform and Twin Support Vector Machine for Pathological Brain Detection.* Applied Sciences, 2016. **6**(6): Article ID. 169

[19] Zhan, T.M. and Y. Chen, *Multiple Sclerosis Detection Based on Biorthogonal Wavelet Transform, RBF Kernel Principal Component Analysis, and Logistic Regression.* IEEE Access, 2016. **4**: p. 7567-7576

[20] Lu, S., *A Pathological Brain Detection System based on Extreme Learning Machine Optimized by Bat Algorithm.* CNS & Neurological Disorders - Drug Targets, 2017. **16**(1): p. 23-29

[21] Zhao, G. *Smart Pathological brain detection by Synthetic Minority Oversampling Technique, Extreme Learning Machine, and Jaya Algorithm*. Multimedia Tools and Applications, 2017, DOI: 10.1007/s11042-017-5023-0.

[22] Muhammad, K. *Ductal carcinoma in situ detection in breast thermography by extreme learning machine and combination of statistical measure and fractal dimension*. Journal of Ambient Intelligence and Humanized Computing, 2017, DOI: 10.1007/s12652-017-0639-5.

[23] Sun, Y., *A Multilayer Perceptron Based Smart Pathological Brain Detection System by Fractional Fourier Entropy.* Journal of Medical Systems, 2016. **40**(7): Article ID. 173

[24] Wang, S.-H. *Single slice based detection for Alzheimer's disease via wavelet entropy and multilayer perceptron trained by biogeography-based optimization*. Multimedia Tools and Applications, 2016, DOI: 10.1007/s11042-016-4222-4.

[25] Ji, G., *Fruit classification using computer vision and feedforward neural network.* Journal of Food Engineering, 2014. **143**: p. 167-177

[26] Wei, L., *Fruit classification by wavelet-entropy and feedforward neural network trained by fitness-scaled chaotic ABC and biogeography-based optimization.* Entropy, 2015. **17**(8): p. 5711-5728

[27] Liu, A.J., *Tea Category Identification using Computer Vision and Generalized Eigenvalue Proximal SVM.* Fundamenta Informaticae, 2017. **151**(1-4): p. 325-339

[28] Zhou, X.-X., *Comparison of machine learning methods for stationary wavelet entropy-based multiple sclerosis detection: decision tree, k-nearest neighbors, and support vector machine.* Simulation, 2016. **92**(9): p. 861-871

[29] Dong, Z., *Classification of Alzheimer disease based on structural magnetic resonance imaging by kernel support vector machine decision tree.* Progress In Electromagnetics Research, 2014. **144**: p. 171-184

[30] Yang, J., *Identification of green, Oolong and black teas in China via wavelet packet entropy and fuzzy support vector machine.* Entropy, 2015. **17**(10): p. 6663-6682

[31] Lu, H.M., *Facial Emotion Recognition Based on Biorthogonal Wavelet Entropy, Fuzzy Support Vector Machine, and Stratified Cross Validation.* IEEE Access, 2016. **4**: p. 8375-8385

[32] Li, Y. and C. Cattani, *Detection of Dendritic Spines using Wavelet Packet Entropy and Fuzzy Support Vector Machine.* CNS & Neurological Disorders - Drug Targets, 2017. **16**(2): p. 116-121

[33] Soda, K.J., D.E. Slice, and G.J.P. Naylor, *The use of geometric morphometrics and artificial neural networks to identify teeth to species in requiem sharks (Carcharhinus sp.).* Integrative and Comparative Biology, 2013. **53**: p. E372

[34] 34. Du, S., *Alzheimer's Disease Detection by Pseudo Zernike Moment and Linear Regression Classification.* CNS & Neurological Disorders - Drug Targets, 2017. **16**(1): p. 11-15

[35] Lv, Y.-D., *Alcoholism detection by data augmentation and convolutional neural network with stochastic pooling.* Journal of Medical Systems, 2018. **42**(1): Article ID. 2

[36] Han, L., *Identification of Alcoholism based on wavelet Renyi entropy and three-segment encoded Jaya algorithm.* Complexity, 2018. **2018**: Article ID. 3198184.